

Thermal response of steel structures to fire: test versus field conditions

Kevin J LaMalva

Simpson Gumpertz & Heger Inc., Waltham, MA, USA

Abstract

This article examines the influence of thermal boundary conditions used for the standard fire resistance test compared to those, which naturally exist in actual building construction. Two protected structural steel assemblies that vary in connection proximity to columns are analyzed. Using finite element modeling, the two assemblies are exposed to a simulated uncontrolled office fire with varying thermal boundary conditions. The modeling results demonstrate an acute effect that heat dissipation may have on the steel temperature distribution of a given structural assembly in an actual application.

Keywords

Structural fire safety, fire resistance, performance based design, heat transfer, structural steel

Introduction

For prescriptive structural fire protection, building codes generally rely on assembly performance as measured directly by furnace testing per requirements of ASTM E 119 [1]. Furnace testing can measure comparative performance of structural assemblies under controlled conditions. However, this testing does not incorporate all factors required for fire hazard or fire risk assessment of the materials, products, or assemblies under actual fire conditions.

The ASTM E 119 standard does not purport to address all safety concerns, if any, associated with its use. It is the responsibility of the user of this standard to establish appropriate practices and determine the applicability of its limitations prior to use [1]. As such, application of standard furnace test results to predict

Corresponding author:

Kevin J LaMalva, Simpson Gumpertz & Heger Inc., Waltham, MA 02453, USA

Email: kjlamalva@sgh.com

the performance of actual building construction requires the evaluation of test conditions.

For performance-based structural fire protection, the engineer-of-record must understand the limitations of standard test conditions with relation to the given application and performance objectives. For example, the engineer must be aware of the differences in temperature distributions in a mock-up structural assembly tested in a furnace and the corresponding full-scale assembly in service. Unfortunately, temperature distribution data for full-scale structural assemblies under fire exposure are relatively limited.

Since the events of September 11, 2001, the engineering community has heightened its focus on structural fire protection requirements for buildings. To support the movement toward performance-based design and rational engineering of structural fire protection, the population of reliable data for calibration and verification should be expanded. It is the author's hope that the modeling results described herein will help to advance the understanding of *in situ* structural steel temperature distributions under fire exposure.

Standard test conditions

The test methods prescribed by the ASTM E 119 standard were first published in 1918, and have remained relatively unchanged to the present day. As part of the testing regime, the standard establishes spot and average threshold steel temperatures that are approximately between 600°C and 700°C [1]. In conjunction with the ability to remain stable during testing, the fire resistance rating that a structural assembly receives is determined in part by its heating characteristics.

In the standard furnace test, individual structural elements are tested in isolation, and connections to supporting members are not included. Structural elements are seated within the furnace so their entire length is uniformly heated. As a result, structural specimens are unable to dissipate heat, as they are likely to do in building construction by interconnection to cooler adjacent structural elements. This article describes thermal models that investigate the effect of such thermal boundary conditions on structural fire performance.

Related research

Understanding the heating characteristics of a structure is a requisite to analyzing its performance under fire exposure. As such, researchers have performed thermal modeling to help understand how structures transfer heat during fire exposure. 2D thermal modeling has been used to analyze the distribution of temperature within structural cross-sections, and 3D thermal modeling has been used to help understand the heating of structures in a global sense. The effect of the removal of spray-applied fire resistive material (SFRM) on the heating of underlying structural steel has also been studied.

As part of their investigation of the World Trade Center 7 (WTC 7) building collapse, the US National Institute of Standards and Technology (NIST) conducted both 2D and 3D thermal analyses. For example, NIST used a 2D thermal model to estimate the temperature history of a protected steel column exposed to a uniform temperature of 1100°C. Additionally, NIST conducted 3D thermal modeling to estimate the thermal state of multiple floors under fire exposure. The temperatures derived from the 3D thermal modeling were spatially averaged over 1 m (3.3 ft) for input into a 3D structural model [2].

The loss of SFRM from structural steel can adversely affect its performance under fire exposure. To help address this issue, Ryder et al. [3] analyzed the effect of the loss of SFRM on the thermal response of steel columns. In their study, 3D thermal modeling was used to estimate the temperature rise within a steel column with varying sections of SFRM removed (e.g., 770 mm² area of SFRM is removed from the column flange). It was found that a more massive column will, to some extent, be able to better withstand the removal of SFRM due to its increased thermal capacity [3].

Thermal modeling

Two protected structural steel assemblies (Assemblies A and B) that vary in connection proximity to columns are analyzed. Assembly A has a girder-to-column double knife plate connection. This structural steel assembly has the primary connection positioned close to the column. The column is modeled as extending for one story above and one story below the modeled girder, which is represented with boundary conditions for symmetry at mid-span. Filler beams are neglected for the analysis since prior research [4] suggests that their effect on the thermal distribution is secondary.

Assembly B utilizes a cantilever beam framing technique with a double shear tab connection located away from the column. The cantilever beam framing technique is described in a section below. Filler beams are also neglected for this assembly.

Each assembly is analyzed under three different conditions: fire below the slab with a column present, fire above and below the slab with a column present, and fire below the slab without a column. The first and second conditions are meant to simulate thermal conditions that may occur in service. The third condition is meant to simulate thermal conditions, which would exist in a furnace test of a structural floor system.

Assembly A structural configuration

Assembly A consists of the following structural components:

- Column: W14X665 (3.9 m (12 ft. – 9 in.) story height)
- Girder: W33X130 (length to mid-span: 6.9 m (22 ft. – 6 in.))
- Lightweight Concrete Slab: 102 mm (4 in.) thick

- Double Knife Plates: 635 mm (25 in.) × 89 mm (3.5 in.) × 9.5 mm (3/8 in.) (each)

The double knife plates are modeled as welded to the column web face. Bolts connecting the girder to the knife plates are not modeled explicitly since prior research [4] suggest that their effect on the thermal distribution is secondary. Figure 1 illustrates the structural configuration of Assembly A.

Assembly B structural configuration

Assembly B consists of the following structural components:

- Column: W14X665 (3.9 m (12 ft. – 9 in.) story height)
- Girder Stem: W33X130 (stem length: 2.1 m (7 ft.))
- Girder (Drop-in Span): W24X104 (length to mid-span: 4.7 m (15 ft – 6 in.))
- Lightweight Concrete Slab: 102 mm (4 in.) thick
- Double Shear Tabs: 368 mm (14–1/2 in.) × 172 mm (6–3/4 in.) × 9.5 mm (3/8 in.) (each)

The girder stem is modeled as welded to the column web face. The two shear tabs connect the drop-in span of the girder to the girder stem. Similar to Assembly A, the bolts likely to be used to connect the drop-in span to the girder stem are not modeled explicitly. Figure 2 illustrates the structural configuration of Assembly B.

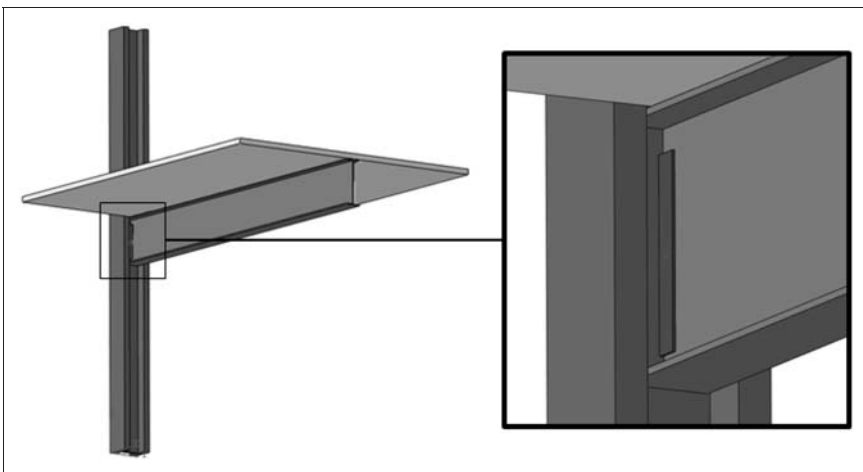


Figure 1. Assembly A structural configuration.

Cantilever framing system

The cantilever framing system used for Assembly B represents a reasonable and economical alternative to simple span and continuous beam framing systems. The primary advantages of such a system are economy, stiffness, and ease of erection. Larger bays and longer spans tend to increase the advantage of using such a system [5].

In terms of economy, cantilever framing systems often have drop-in sections that are shallower than the stem sections, thereby reducing the total steel weight and cost. In terms of stiffness, a typical cantilever system designed on the basis of flexural strength typically has about half the deflection of an equivalent simple span system and is almost as stiff as a continuous beam system. Compared to continuous framing, a cantilever beam is more forgiving to erect because small errors in the length of support columns are easily accommodated [5].

Applied fire protection

SFRM helps to delay the transmission of heat from a fire to the structural steel. Characteristic of the structural fire protection used for WTC 7 [2], the thicknesses of the gypsum-based SFRM are modeled as follows [2]:

- Column: 22 mm (7/8 in.; 3-hr rating)
- Girder/Girder Stem: 13 mm (1/2 in.; 2-hr rating)
- Concrete Slab (underside): 9.5 mm (3/8 in.; 2-hr rating)
- Knife Plates/Shear Tabs: 13 mm (1/2 in.; assumed same as girder)

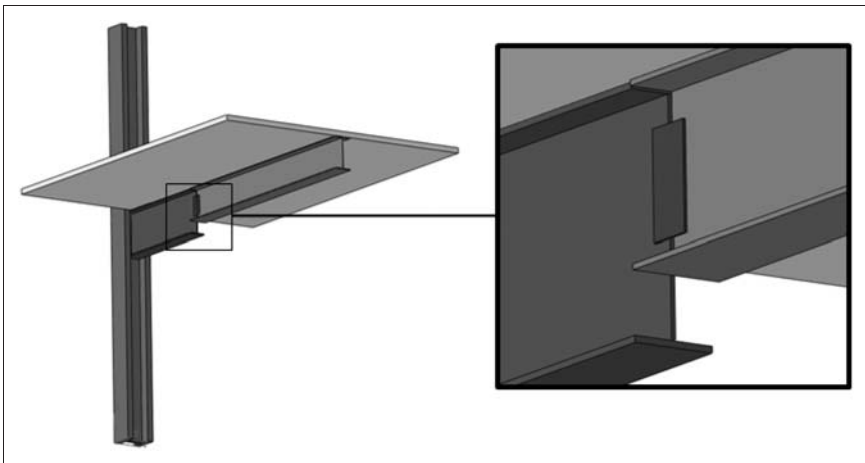


Figure 2. Assembly B structural configuration.

Fire exposure

The upper gas layer temperature history characteristic of an uncontrolled office fire [4] is used for the analyses. Figure 3 compares this gas temperature history to that estimated for WTC 7 [2]. Whereas the gas temperature history from the northeast corner of WTC 7 represents the spread of fire around a central building core, the history used for the analyses contained herein represents a fire that grows radially and has less available oxygen to support combustion.

Material thermal properties

The density of steel, lightweight concrete, and SFRM are taken to be 7850 kg/m^3 (490 pcf), 1522 kg/m^3 (95 pcf), and 256 kg/m^3 (16 pcf) [2], respectively, all of which remain nearly constant with temperature. The conductivity and specific heat of lightweight concrete are fairly constant with temperature and are taken to be $0.80 \text{ W/(m } ^\circ\text{C)}$ and $840 \text{ J/(kg } ^\circ\text{C)}$, respectively [6]. The conductivity and specific heat of steel [6] and the gypsum-based SFRM [2] are dependent upon temperature as shown in Figure 4 and Figure 5.

Heat transfer simulation

Abaqus/Standard is used to perform transient heat transfer analyses, which include solid body heat conduction, convection and radiation boundary conditions, and

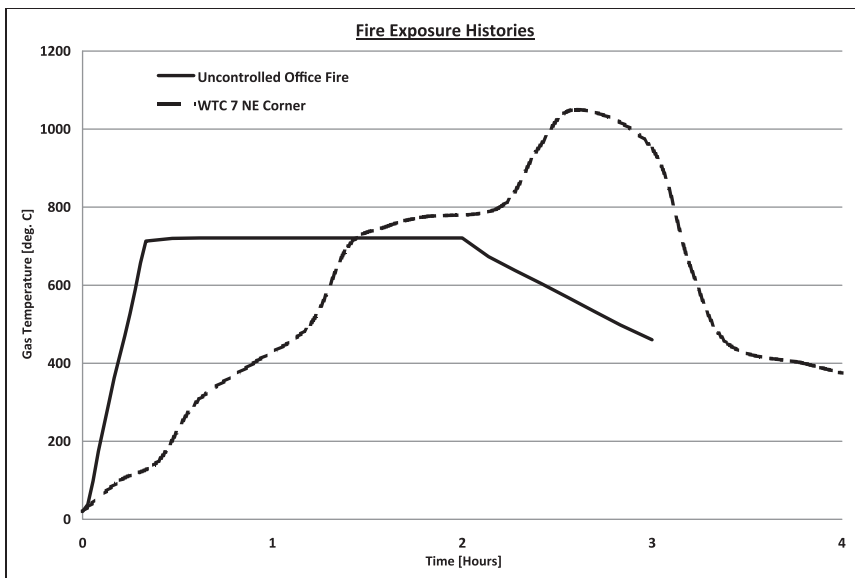


Figure 3. Fire exposure histories.

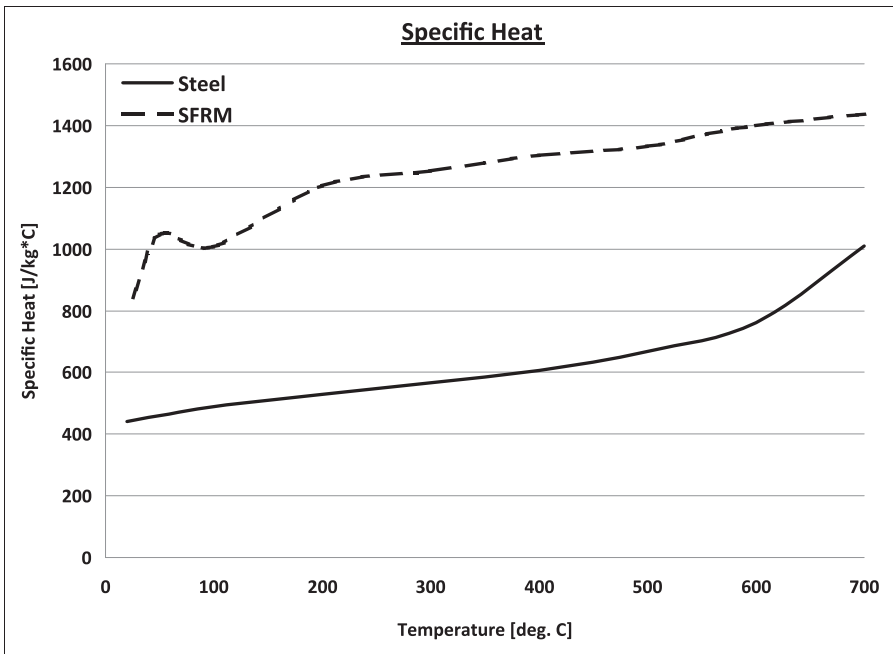


Figure 4. Temperature-dependent specific heat.

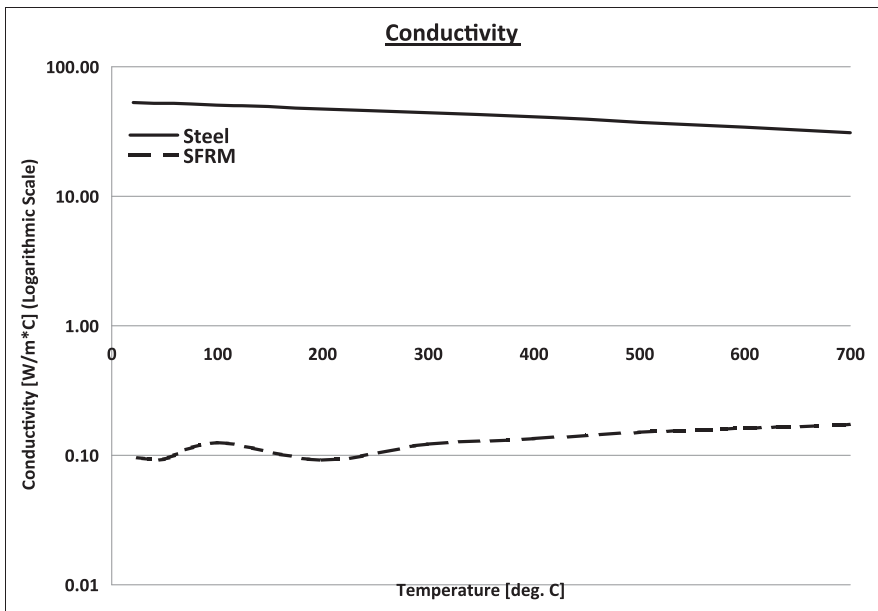


Figure 5. Temperature-dependent conductivity.

temperature-dependent thermal properties of the materials. Hexahedral, structured, linear, heat transfer elements (DCC3D8: 8-node convection/diffusion brick) are used to mesh all components of the model [7]. The model contains three materials (steel, SFRM, and lightweight concrete) with thermal properties described above. The steel and lightweight concrete components are covered with SFRM to the thicknesses described above. Thermal contact definitions are assigned to specific regions of the model to allow conduction heat transfer between components in direct contact (e.g., contact between the girder top flange and the concrete slab).

Turbulent natural convection and radiation are the modes of heat transfer to the structural assembly during the fire exposure. The convection heat transfer coefficient is specified as $25 \text{ W}/(\text{m}^2 \text{ }^\circ\text{C})$ [6] and the exposure temperature history is that shown in Figure 3 for an uncontrolled office fire. Radiation between the structural assembly and the exposure atmosphere is represented in the model with reference to the office fire temperature history. The emissivity of the structural assembly is assumed to be 0.9.

Convection and radiation heating is applied to the exposed outside surfaces of the SFRM covering the column, girder, slab, and connection components. The column is exposed to fire on all four of its sides. For the two-floor fire exposure, the column height above the floor and the exposed top face of the concrete slab are included in the surfaces of fire exposure involvement. The outer boundaries of the model are assumed to be adiabatic. Figure 6 to 8 illustrate the Assembly A and Assembly B thermal models.

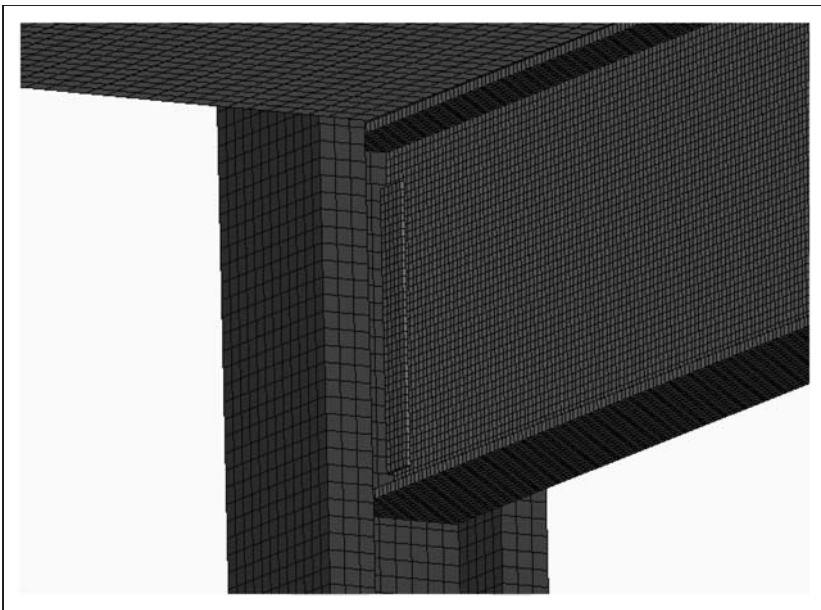


Figure 6. Assembly A thermal model (double knife plate connection; SFRM not shown).

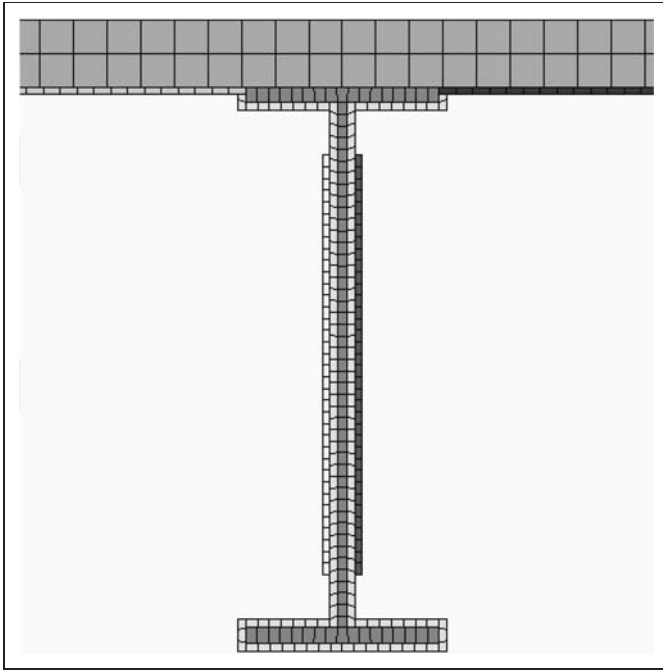


Figure 7. Assembly A thermal model (elevation view; column not shown).

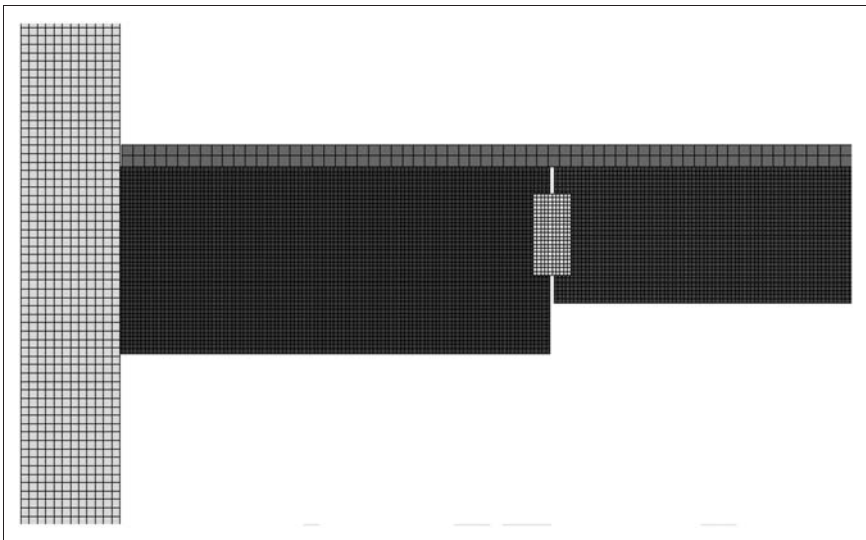


Figure 8. Assembly B thermal model (elevation view; SFRM not shown).

Thermal modeling results

Figure 9 to 12 compare the temperature histories of select assembly locations for each of the three fire exposure conditions analyzed. Table 1 summarizes key observations drawn from the thermal modeling results. The concrete slab and the protected column act as heat sinks in both the Assembly A and Assembly B models. For example, the top flange of the girder attains a lower temperature than the bottom flange due to the heat sink effect of the slab.

The concrete slab has a relatively high specific heat resulting in slower heating with relation to the steel. The resulting temperature gradient between the steel and concrete slab drives thermal conduction toward the slab. This behavior is consistent with structural fire design guidance in Eurocode 3, which provides equations for vertical nonuniform temperature profiles of steel beams supporting a concrete slab under fire exposure [8].

The ability of the concrete slab to act as a heat sink is reduced when the two-story fire condition is considered since the exposure of the unprotected top face of the slab results in higher slab temperatures. The increase in temperature of the concrete slab reduces the temperature gradient between it and the steel below resulting in less heat dissipation. The reduction in the heat sink ability of the concrete slab for the two floor fire case does not affect the temperature history of either the girder web or bottom flange.

The column is structurally robust for high-rise application and is protected with SFRM rated for 3-hr protection. As a result, the column maintains relatively low

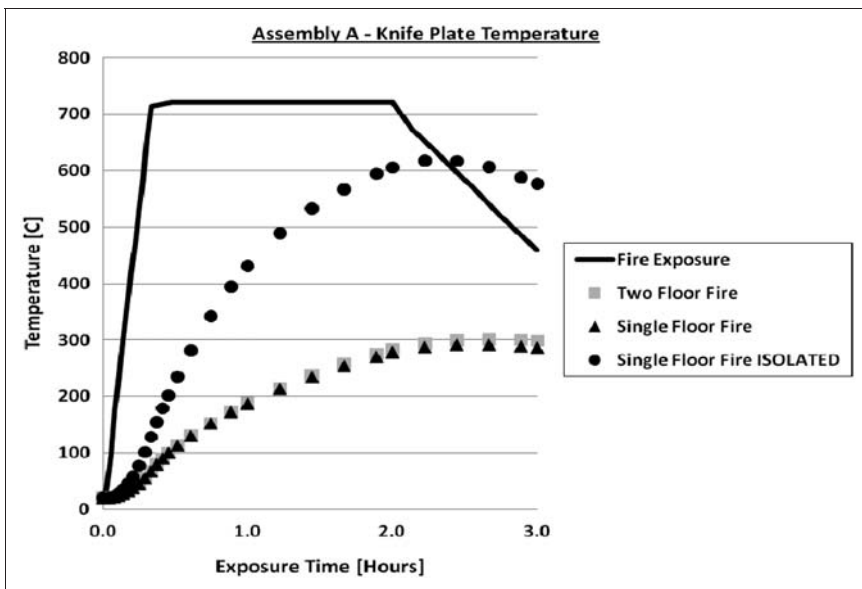


Figure 9. Assembly A knife plate temperature histories.

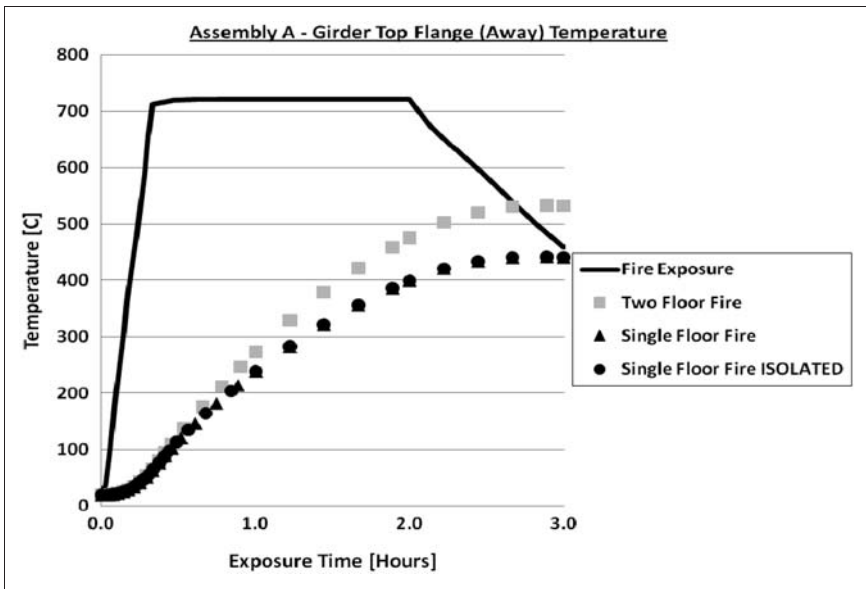


Figure 10. Assembly A girder top flange temperature histories (4 ft. away from column).

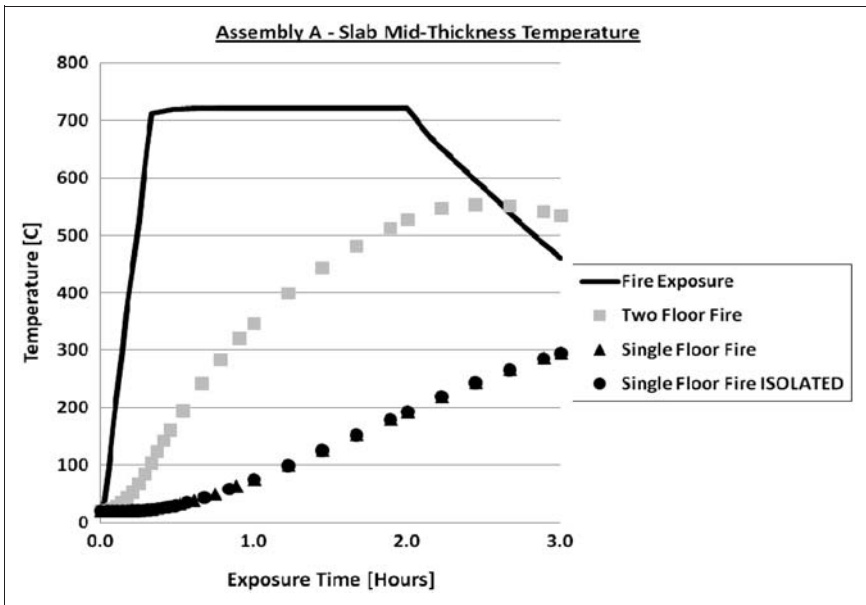


Figure 11. Assembly A slab mid-thickness temperature histories.

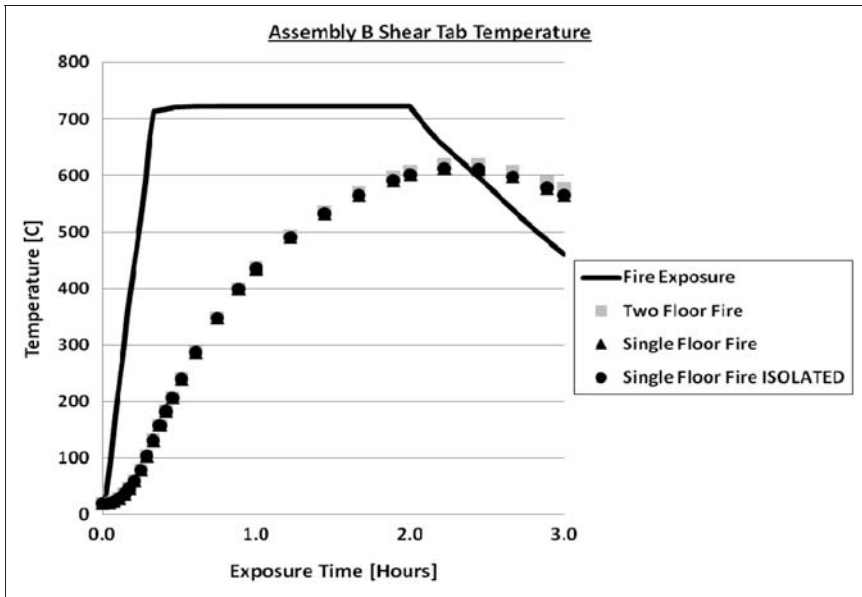


Figure 12. Assembly B shear tab temperature histories.

Table 1. Key observations of thermal modeling results.

Comparison	Observation
Single floor fire versus two floor fire (Assembly A and B)	Girder top flange heats up faster in two floor fire Girder bottom flange heats up equally in both cases Girder web heats up equally in both cases Slab mid-thickness heats up faster in two floor fire
Column versus no column (Assembly A)	Knife plates heat up much faster in no-column case
Column versus no column (Assembly B)	Shear tabs heat up equally in both cases

temperatures in relation to the other steel components. The low temperatures that are maintained by the column during fire exposure drive thermal conduction toward the column.

For Assembly A, the heat sink effect of the protected column acts to cool the knife plates. For the condition in which the column is not present for Assembly A, the knife plates heat up faster and reach significantly higher temperatures during the fire exposure.

For Assembly B, the heat sink effect of the protected column does not appreciably reduce the temperature of the shear tabs. As such, the shear tabs experience nearly identical temperature histories whether the column is present or not. This occurs because heating of the girder stem which separates the shear tabs from the protected column acts to drastically reduce the temperature gradient, limiting the heat dissipation via conduction from the shear tabs.

The thermal modeling results of Assembly A assume ideal thermal contact between the knife plates and the column, and between the knife plates and the girder. Since the knife plates are welded to the column, ideal thermal contact is an accurate assumption. However, the bolts that would connect the knife plates to the girder may not produce ideal thermal contact in application. As a sensitivity check to this, the thermal contact areas between the girder and knife plates are geometrically reduced by 50%. This reduction in contact area does not appreciably change the resulting temperature distributions at either the girder (bolt region) or the knife plates (no more than a 7% change at any time during the fire exposure).

Discussion of results

Since steel connections are not included in standard testing, information on their heating characteristics is scarce. This is in spite of connection failures contributing to the collapse of protected steel structures due to fire exposure. NIST reported that failure of seated connections contributed to the global collapse of WTC 7 due to fire exposure [2]. Additionally, the internal collapse of WTC 5 was initiated by the failure of shear tab connections [4].

The steel connection of Assembly A is directly at the column. As a result, the knife plates of Assembly A experience significantly lower temperatures than would be realized during a standard test. This occurs because the protected column acts as an effective heat sink. The steel connection of Assembly B is located 2.1 m (7 ft.) away from the column. As a result, the shear tabs of Assembly B experience temperatures, which are relatively similar between the field and test condition exposure scenarios. In this case, the connection becomes thermally isolated from the column and cannot effectively dissipate heat, which mimics standard test conditions

For Assembly A, the presence of the protected column functioning as a heat sink helps to maintain the temperature of the knife plates below 350°C. When the protected column is excluded from Assembly A, the knife plates reach temperatures in excess of 600°C. For Assembly B, the shear tabs reach temperatures in excess of 600°C whether a column is present or not.

A36 steel is a standard alloy commonly used for structural applications in the USA. Figure 13 plots the strength behavior of A36 steel as a function of temperature [9]. At 320°C, A36 steel actually possesses a higher ultimate strength than it has at ambient temperature due to heat treating effects (i.e., hardening due to temperature). At 600°C, A36 steel only possesses approximately 40% of its ultimate strength compared to its ambient condition. Consideration of these strength characteristics demonstrates the tremendously beneficial heat dissipation role that a

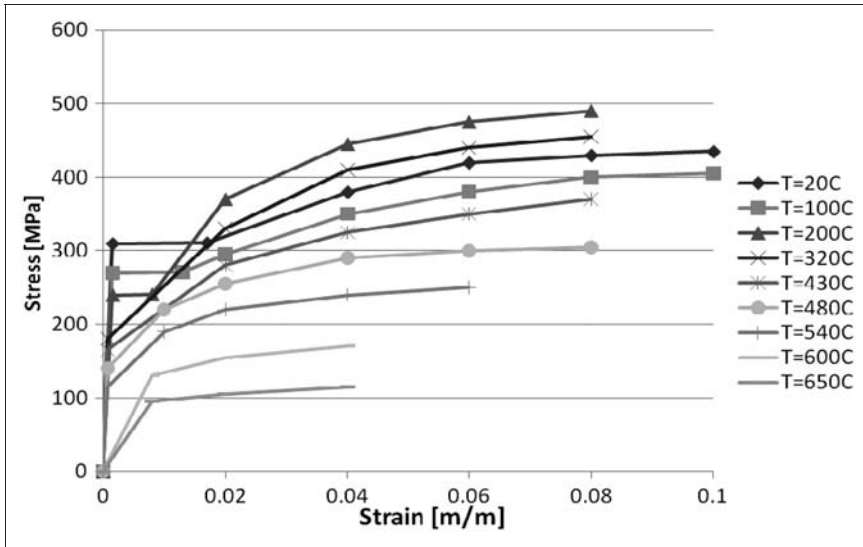


Figure 13. Temperature-dependent A36 steel strength behavior.

protected column may offer to a structural assembly. For Assembly B, the benefits of effective heat dissipation from the shear tabs is unfortunately not realized due to its geometric configuration. This leads to shear tabs temperatures that are very similar to the girder mid-span, not to mention similar to the results that standard testing would demonstrate.

Conclusions

Standard fire resistance testing provides a convenient method of establishing a rank ordering of different structural assemblies under controlled laboratory conditions. These standard tests help to uphold a high level of quality in building construction, and there is no question that the good practices incorporated into prescriptive standards significantly raise the level of fire safety in buildings. However, the level of risk associated with code compliance for fire protection remains unquantifiable [10].

The standard furnace test establishes spot and average threshold steel temperatures that are approximately between 600°C and 700°C for test procedures of structural members [1]. In application, steel temperatures lower than 600°C may cause connection failure (e.g., as reported for WTC 7 and WTC 5). When the column acts as an effective heat sink (e.g., Assembly A), the temperature of critical connection regions may be reduced compared to the corresponding test condition. Yet, in some cases (e.g., Assembly B) such a reduction from theoretical test temperatures does not occur.

The standard furnace test is predicated on the assumption that the test assembly is representative of actual field construction to a certain extent. Protecting structures with the narrow focus of meeting prescriptive code requirements for fire resistance may overlook inherent weaknesses of the *in situ* condition of a given structural assembly. Alternatively, it can also result in the dismissal of inherent strengths that may justify less applied protection.

The testing regime for the assemblies examined would be relatively similar according to standard test requirements. Yet, the thermal modeling results described above demonstrate that the connection region of each assembly may develop very different temperatures, potentially impacting performance during a fire. For performance-based structural fire protection, the engineer must be aware of the differences in temperature distribution among a mock-up structural assembly tested in a furnace and the corresponding full-scale assembly used in an application.

References

1. ASTM E 119-07a. *Standard test methods for fire tests of building construction and materials*. West Conshohocken, PA: ASTM International, 2007.
2. NIST. *Final report on the collapse of World Trade Center Building 7*. Gaithersburg, MD: National Institute of Standards and Technology, 2008.
3. Ryder NL, Wolin SD and Milke JA. An investigation of the reduction in fire resistance of steel columns caused by loss of spray applied fire protection. *Journal of Fire Protection Engineering* 2002; Vol. 12: No. 1.
4. LaMalva KJ, Barnett JR and Dusenberry DO. Failure analysis of the World Trade Center 5 building. *Journal of Fire Protection Engineering* 2009; Vol. 19: No. 4.
5. Hemstad M. Cantilever beam framing systems. *Engineering Journal* 1999; 3rd Quarter.
6. Buchanan AH. *Structural design for fire safety*. Hoboken, NJ: John Wiley & Sons, 2002.
7. Abaqus. *Abaqus analysis manual (Version 6.10)*. Providence, RI: Simulia, Dassault Systèmes, 2010.
8. Eurocode 3: Design of steel structures – Part 1-2: General rules – Structural fire design (BS EN 1993-1-2: 2005), European Committee for Standardization (CEN).
9. Harmathy TZ. *Fire safety design and concrete*. London: Longman Scientific and Technical, 1993.
10. Fitzgerald RW. *Building fire performance analysis*. Hoboken, NJ: John Wiley & Sons, 2004.